ACOUSTIC SIGNALS PROCESSING. COMPUTER SIMULATION

A Low-complexity Minimum Variance Algorithm Combined with Power Method for Ultrasound Imaging

Ping Wang[a], *, Tingting Du[a], Linhong Wang[b], Lu Kong[a], Xitao Li[a], and Yizhe Shi[c]

[a]State Key Lab. of Power Transmission Equip. and System Security and New Tech., Chongqing University, Chongqing, 400044 China
[b]Chongqing College of Electronic Engineering, Chongqing, 401331 China
[c]State Grid Fujian Electric Power Co., Ltd., Maintenance Branch, Fujian, 350003 China
*e-mail: cqu_dqwp@163.com

Abstract—Aiming at the problem of high complexity and poor real-time performance of the traditional minimum variance (MV) algorithm, a low-complexity minimum variance algorithm combined with power method is proposed. Firstly, the echo data is transformed into beam domain by discrete cosine transform and the dimension reduction parameter is determined according to the data of scanning lines. Secondly, the maximum eigenvalue and corresponding eigenvector of sample covariance matrix are obtained by the power method to reduce the complexity of eigenvalue decomposition. Finally, by ignoring low-energy echo signal, the inversion of covariance matrix can be simplified to construct a new weighted vector, which can reduce the complexity of MV. The Field II simulation results show that the proposed algorithm has better resolution, contrast ratio and efficiency than the traditional MV algorithm, and outperforms the minimum variance algorithm based on eigenvalue decomposition (ESBMV) in resolution and efficiency.

1. INTRODUCTION

Ultrasound imaging system mainly includes transmitting, receiving, beamforming and imaging modules [1]. The beamforming module is the core of the whole system, which directly determines the imaging quality [2]. The traditional delay and sum (DAS) is the simplest and most widely used algorithm in ultrasound imaging beamforming [3, 4]. However, the DAS algorithm has poor performance in resolution and contrast ratio, so the adaptive beamforming technology is proposed in recent years [5–8]. The typical adaptive beamforming method includes the minimum variance algorithm (MV) [9] and the generalized sidelobe canceller (GSC) algorithm [10, 11]. The idea of MV is to minimize the output power of beamformer while keeping the total gain constant, so as to reduce the interference signals in unexpected directions and obtain the optimal weighted vector [12, 13]. Based on the minimum power distortion response beamformer, the GSC is proposed to minimize the output power and suppress residual noise [14, 15].

Compared with the traditional DAS algorithm, adaptive beamforming algorithms can significantly improve the resolution and contrast ratio [16]. However, adaptive algorithms need to calculate the dynamic weighting vectors in real time, which involve complex matrix operations [17]. The high complexity seriously affects the real-time performance of adaptive algorithms and reduces the robustness. Therefore, many scholars are committed to reduce the complexity of adaptive algorithm. Fuhrmann used Toeplitz matrix to construct sample covariance matrix, and simplified the matrix inversion to decrease the complexity of adaptive algorithms [18]. Park et al. proposed the fast inversion of sample covariance matrix using QR decomposition technique [19]. Kim et al. utilized Principal Component Analysis (PCA) to extract the eigenvectors corresponding to the larger eigenvalues in the covariance matrix to form the dimension reduction matrix [20, 21]. The adaptive space-time reduced-rank interference suppression least squares algorithm based on joint iterative optimization of parameter vectors was proposed to solve the optimal basic set of reduced-rank processing [22]. Albulayli put forward a hybrid adaptive and non-adaptive algorithm to reduce the computation of adaptive algorithms [23]. The Low complex subspace MV beamformer ignored part of the row data in original covariance matrix, but the covariance matrix was not a square matrix [24].

To further reduce the complexity of traditional MV algorithm, a low-complexity minimum variance algo-

rithm (LCMV) combined with power method was proposed in this paper. Firstly, the dimension of covariance matrix is reduced by discrete cosine transform (DCT) according to the scanning lines data. Secondly, the largest eigenvalue and its corresponding eigenvector are extracted by power method while some low-energy signal data are ignored. Lastly, the matrix inversion is simplified to vector multiplication which greatly reduces the complexity. Besides, Field II [25] is introduced to inspect the effectiveness of the proposed algorithm.

This paper is organized as follows: section 2 reviews the MV, minimum variance algorithm based on eigenvalue decomposition (ESBMV) briefly and introduces the proposed LCMV in detail. In section 3, the point targets and cyst phantom are simulated, the point target with different center frequencies and the complexity of different algorithms are also compared and analyzed. The conclusion is drawn in section 4.

2. METHOD

2.1. Minimum Variance Algorithm

Suppose a linear array which consists of N elements, and its beamforming output is given by:

$$\mathbf{y}(k) = \mathbf{w}^H(k)\mathbf{x}_d(k) = \sum_{i=1}^{N} \mathbf{w}_i(k)\mathbf{x}_i(k - \Delta_i), \qquad (1)$$

where k is the k-th sampling point. $\mathbf{x}_d(k) = [x_1(k - \Delta_1), \ldots, x_N(k - \Delta_N)]^T$ is the echo data after focus delay, and Δ_i is the delay time applied to each element signal, $[\cdot]^T$ is the transposition operation. $\mathbf{w}(k) = [w_1(k), \ldots, w_N(k)]^T$ is the adaptive weighting vector, and $[\cdot]^H$ is the conjugate transposition operation.

According to the principle of MV, the solution of the weighting vector is:

$$\min_{w} \mathbf{w}^H \mathbf{R} \mathbf{w}, \quad subject\ to\ \mathbf{w}^H \mathbf{a} = 1, \qquad (2)$$

where $\min(\cdot)$ is the minimum operation, $\mathbf{R} = E[\mathbf{x}_d \mathbf{x}_d^H]$ is the $N \times N$ sample covariance matrix, and $\mathbf{a} = [1, 1, \cdots, 1]^T$ is the $N \times 1$ direction vector, then the problem (2) can be solved by the Lagrangian multiplier method to obtain the optimal weighting vector $\mathbf{w}_{opt}$:

$$\mathbf{w}_{opt} = \frac{\mathbf{R}^{-1}\mathbf{a}}{\mathbf{a}^H \mathbf{R}^{-1}\mathbf{a}}. \qquad (3)$$

The output of MV is:

$$\mathbf{y}_{mv}(k) = \mathbf{w}_{opt}^H \mathbf{x}_d(k). \qquad (4)$$

2.2. Minimum Variance Algorithm based on Eigenvalue Decomposition

The eigenvalue decomposition of the sample covariance matrix is conducted by:

$$\mathbf{R} = \mathbf{E}_s \mathbf{\Lambda}_s \mathbf{E}_s^H + \mathbf{E}_n \mathbf{\Lambda}_n \mathbf{E}_n^H$$
$$= \sum_{i=1}^{num} \lambda_i \mathbf{e}_i \mathbf{e}_i^H + \sum_{i=num+1}^{N} \lambda_i \mathbf{e}_i \mathbf{e}_i^H, \qquad (5)$$

where $\mathbf{E}_s = [\mathbf{e}_1, \mathbf{e}_2, \ldots, \mathbf{e}_{num}]$ is the signal subspace, num is the dimension of signal subspace, $\mathbf{E}_n = [\mathbf{e}_{num+1}, \mathbf{e}_{num+2}, \ldots, \mathbf{e}_N]$ is the noise subspace. $\mathbf{e}_i(i = 1, 2, \cdots, N)$ are the eigenvectors corresponding to the N eigenvalues $\lambda_i(i = 1, 2, \ldots, N)$ of sample covariance matrix, which satisfy $\lambda_1 \geq \lambda_2 \geq \ldots \geq \lambda_N$. $\mathbf{\Lambda}_s = \mathrm{diag}\{\lambda_1, \lambda_2, \ldots, \lambda_{num}\}$ and $\mathbf{\Lambda}_n = \mathrm{diag}\{\lambda_{num+1}, \lambda_{q+2}, \ldots, \lambda_N\}$ are the diagonal matrices composed of corresponding eigenvalues. The optimal weighting vector $\mathbf{w}_{esbmv}$ can be obtained by projecting the MV weighting vector into the signal subspace:

$$\mathbf{w}_{esbmv} = \mathbf{E}_s \mathbf{E}_s^H \mathbf{w}_{opt} = \mathbf{E}_s \mathbf{E}_s^H \frac{\mathbf{R}^{-1}\mathbf{a}}{\mathbf{a}^H \mathbf{R}^{-1}\mathbf{a}}. \qquad (6)$$

Although ESBMV is obviously improved in resolution and contrast ratio, it involves the computationally expensive operation of eigenvalues and eigenvectors.

2.3. Low-complexity Minimum Variance Algorithm based on Power Method

The DCT is often used to construct the $(1 + p) \times L$ transformation matrix, where L is the size of subarray, p is the dimension reduction parameter. The transformation matrix is as follows:

$$\mathbf{T}_{k,n}$$
$$= \begin{cases} \dfrac{1}{\sqrt{L}}, & k = 0, 0 \leq n \leq L - 1, \\[2mm] \dfrac{2}{\sqrt{L}}\cos\left(\dfrac{\pi k\left(n + \dfrac{1}{2}\right)}{L}\right), & 1 \leq k \leq p,\ 0 \leq n \leq L - 1. \end{cases} \qquad (7)$$

The matrix $\mathbf{T}$ satisfies $\mathbf{T}\mathbf{T}^H = I$, where I is the unit matrix. The selection of p is based on the principle of minimizing the distortion to ensure the imaging quality of LCMV algorithm, which satisfies $2 < (p + 1) < L$. With the increase of p, the result is closer to the original image, but the dimension of covariance matrix is also increased, which raises the complexity. Therefore, the mean square error (MSE) is introduced, which is defined as:

$$\mathrm{MSE} = \frac{1}{WH}\sum_{i=1}^{W}\sum_{j=1}^{H}(r(i,j) - \hat{r}(i,j))^2, \qquad (8)$$

where $r(i, j)$ is the original image element, $\hat{r}(i, j)$ is the transformed image element, i, j are the variables of length and width, and W, H are the length and width of the image respectively. The result will be better when MSE is smaller. See section 3.4 for the specific selection of p.

Since the echo signal of spatially-smoothed array is multiplied by the transformation matrix $\mathbf{T}$, the echo signal of beam domain can be obtained. The sample covariance matrix is gained by extracting the partial beam domain data and the dimension is changed from $L \times L$ to $(p + 1) \times (p + 1)$. So the complexity of matrix inversion after the transformation changes from $O(L^3)$ to $O((p + 1)^3)$. Taking l-th sub-array as an example, the signal is transformed as follows:

$$\mathbf{x}_b^l(k)_{(1+p)\times 1} = \mathbf{T}_{(1+p)\times L} \mathbf{x}_n^l(k)_{L\times 1}, \qquad (9)$$

where $\mathbf{x}_b^l(k)$ is the sub-array signal in beam domain, and the sample covariance matrix is correspondingly changed to:

$$\hat{\mathbf{R}}_b(k) = \frac{1}{N - L + 1} \sum_{l=1}^{N-L+1} \mathbf{x}_b^l(k)_{(1+p)\times 1} \mathbf{x}_b^l(k)^H_{1\times(1+p)} \qquad (10)$$
$$= \mathbf{T}_{(1+p)\times L} \hat{\mathbf{R}}(k) \mathbf{T}^H_{L\times(1+p)}.$$

The proposed LCMV algorithm is simplified by the improved power method for the inversion and the eigenvalue decomposition of the beam domain covariance matrix. The maximum eigenvalue of the covariance matrix and its corresponding eigenvector are obtained by the power method. Set $\mathbf{e}_0 = [1, 1, \ldots, 1]$, the iterative operation is performed as follows:

$$\mathbf{e}_{i+1} = \hat{\mathbf{R}}_b(k) \mathbf{e}_i, \quad \lambda_{i+1} = \max(\mathbf{e}_{i+1}), \qquad (11)$$

where $\mathbf{e}_{i+1}$ is the eigenvector after $(i+1)$-th iteration, and $\max(\cdot)$ is the maximum element solving operation. After every iteration, the obtained vector is normalized into the next iteration. Taking i-th iteration as an example, the vector $\mathbf{e}_i$ is obtained and the normalization process $\mathbf{e}_i = \mathbf{e}_i/\max(\mathbf{e}_i)$ is conducted. Then the iterative operation is repeated by equation (11), and $|\lambda_{i+1} - \lambda_i|/|\lambda_{i+1}| < \varepsilon$ is the end condition of the iterative operation. ε can be selected according to the accuracy requirement, in this paper ε is set to 0.001.

Since the eigenvalues of the covariance matrix represent the energy of the received signal, the signal with large eigenvalue corresponds to strong signal energy. Therefore, some low-energy signals can be ignored to simplify the matrix inversion. The eigenvalues corresponding to noise subspace take the same value when the trace of covariance matrix is invariant, so the energy of ultrasound signal keeps constant:

$$\lambda_{q+1} = \lambda_{q+2} = \ldots = \lambda_{p+1}$$
$$= \frac{1}{p - q + 1}\left(\text{trace}(\hat{R}_b) - \sum_{i=1}^{q} \lambda_i \right), \qquad (12)$$

where $\lambda_{q+1} = \lambda_{q+2} = \ldots = \lambda_{p+1} = [1/(p - q + 1)]$, $\left(\text{trace}(\hat{R}_b) - \sum_{i=1}^{q} \lambda_i \right) = \alpha$, q is the number of the eigenvalues corresponding to signal subspace, the inversion of sample covariance matrix after diagonal loading can be reduced to:

$$\hat{\mathbf{R}}_b^{-1} = \alpha^{-1}\left[I - \sum_{i=1}^{q}\left(\frac{\lambda_i - \alpha}{\lambda_i} \right)\mathbf{e}_i \mathbf{e}_i^H \right]. \qquad (13)$$

In order to further simplify the equation (13), partial beam domain signal can be ignored and set $q = 1$. Then the inversion of covariance matrix is converted into vector multiplication, which can reduce the complexity to $O((p + 1)^2)$:

$$\hat{\mathbf{R}}_b^{-1} = \alpha^{-1}\left[I - \left(\frac{\lambda_1 - \alpha}{\lambda_1} \right)\mathbf{e}_1 \mathbf{e}_1^H \right]. \qquad (14)$$

Only the largest eigenvalue and corresponding eigenvector are used in Eq. (14), that is $\lambda_1 = \lambda_{\max}$, $\mathbf{e}_1 = \mathbf{e}_{\max}$. The maximum eigenvalue $\lambda_{\max}$ and the corresponding eigenvector $\mathbf{e}_{\max}$ are obtained by the iterative processing of the power method. The improved weighting vector $\mathbf{w}_{ib}$ is obtained by substituting Eq. (14) into Eq. (3), and the weighting vector is projected into the eigenvector $\mathbf{e}_{\max}$. According to the orthogonal characteristics between eigenvectors, the noise signal is eliminated and the optimal weighting vector $\mathbf{w}_{ibmv}$ is obtained:

$$\mathbf{w}_{ibmv} = \mathbf{e}_{\max}\mathbf{e}_{\max}^H\mathbf{w}_{ib} = \mathbf{e}_{\max}\mathbf{e}_{\max}^H \frac{\hat{\mathbf{R}}_b^{-1} \mathbf{a}_b}{\mathbf{a}_b^H \hat{\mathbf{R}}_b^{-1} \mathbf{a}_b}, \qquad (15)$$

where $\mathbf{a}_b = \mathbf{T}\mathbf{a}$ is the beam domain direction vector.

3. SIMULATION EXPERIMENTS

In this section, the traditional DAS, MV, ESBMV and proposed LCMV algorithms are simulated with point targets and cyst phantom by Field II. The simulation parameters are listed in Table 1. All the algorithms have used the spatial smoothing and diagonal loading technique.

To inspect the robustness of these algorithms, 10 dB Gauss white noise is added for the inspection. Besides, the point targets simulation is carried out with different center frequencies.

Table 1. Simulation parameters

Parameters	Value
Transducer number, N	64
Subarray length, L	32
Center frequency, f_0/MHz	7
Sampling frequency, f_s/MHz	100
Element pitch, mm	0.11
Element height, mm	5
Sound velocity, m/s	1540
Dynamic range, dB	60

3.1. Point Targets Simulation

15 target points are set in the simulation, and the axial distance is between 30 and 80 mm. Among them, there are 3 point targets at 40 and 60 mm, and 1 target point at other positions. The image results are shown in Fig. 1, from which we can see that DAS owes the worst performance and serious lateral artifacts. The imaging quality of MV improves a little compared with DAS. ESBMV further improves the resolution based on MV and greatly reduces the artifacts. Compared with ESBMV, the proposed LCMV has better resolution and clearer far-field target points. Moreover, 10 dB noise is added to simulate the practical occasions. As shown in Fig. 2, white spots appear in background area, and the contrast becomes worse.

To intuitively investigate the imaging quality of point targets, 3 target points nearest to the focus are selected for lateral resolution analysis. The results are shown in Figs. 3a, 3b. Compared with Fig. 3a, the total energy difference of the echo signal is reduced and the sidelobe is raised in Fig. 3b, which indicates that the

discrimination between the background and the target regions is decreased after adding noises. The mainlobe width at the normalized amplitude of −6 dB and the first sidelobe peak are selected to represent the imaging quality of point targets. Detailed results are shown in Table 2.

From Table 2, the indicators of DAS are apparently worse than adaptive algorithms. No matter whether there is noise or not, the mainlobe width of the proposed LCMV algorithm is better than that of MV and ESBMV. After adding noises, the mainlobe width and sidelobe peak of all algorithms become worse. Compared with MV, the first sidelobe peak of LCMV is reduced by 11.29 and 25.85 dB under noise and non-noise conditions, respectively. Besides, the sidelobe of LCMV is similar to that of ESBMV algorithm.

3.2. Cyst Phantom Simulation

The cyst phantom is set 3 mm radius circular region located at the axial distance of 25 mm in a speckle medium. There are 100 000 noise scattering points randomly distributed in the background area. The imaging results without or with 10 dB noise are shown in Figs. 4 or 5 respectively.

As shown in Fig. 4, compared with adaptive algorithms, the performance of DAS is very poor, and there are obvious white artifacts in the cyst phantom area. The imaging quality of MV is better than that of DAS. Compared with MV, the cyst phantom area of ESBMV and LCMV are darker, and they have better contrast ratio. As shown in Fig. 5, the imaging quality of all algorithms are degraded obviously after adding noise, and detailed results are shown in Tables 3 and 4 respectively. Contrast ratio (CR) is the absolute value of the difference between the mean power of cyst
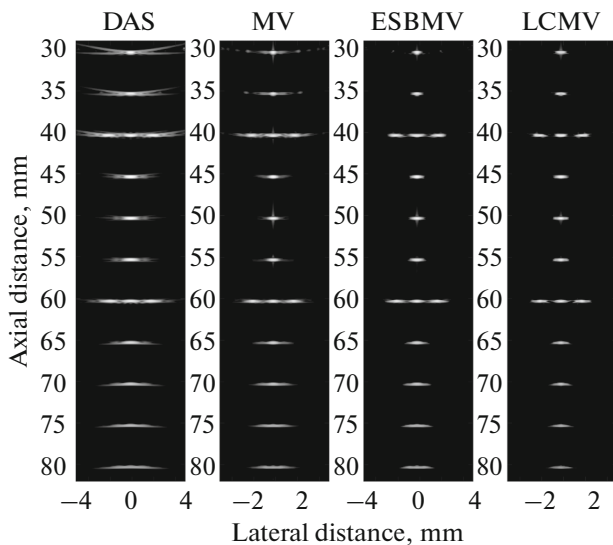
Fig. 1. Point targets imaging without noise.
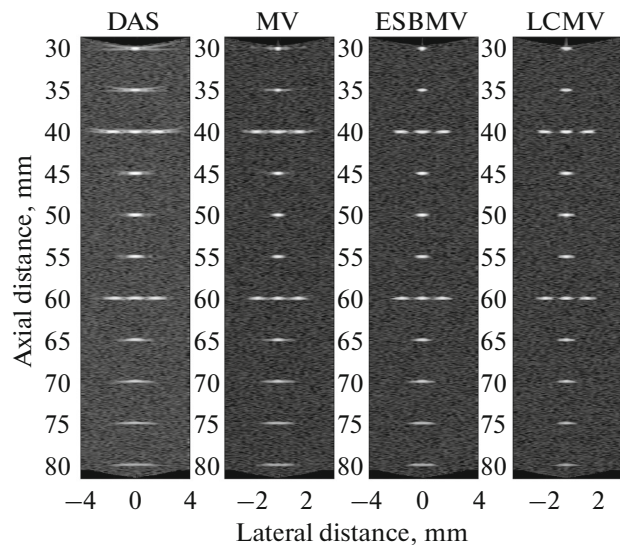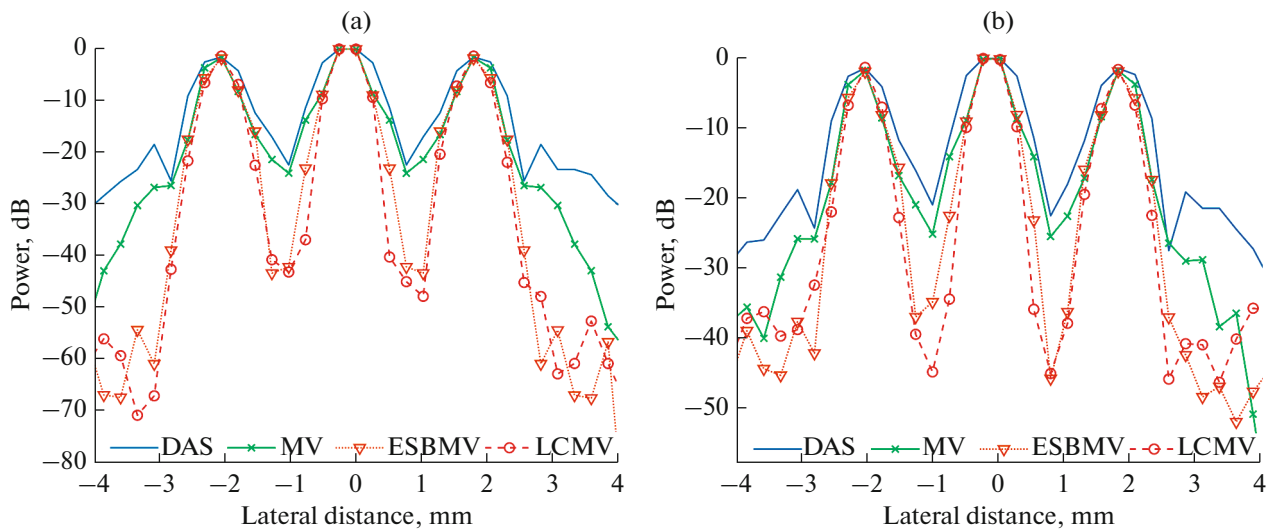

Fig. 2. Point targets imaging with noise.

Fig. 3. (a) The resolution at 40 mm without noise. (b) The resolution at 40 mm with 10 dB noise.
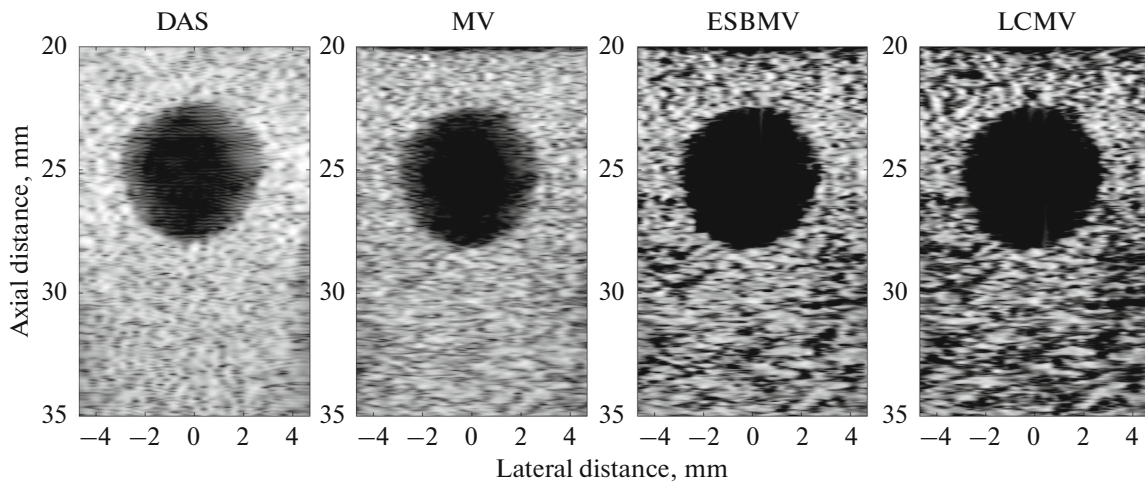

Fig. 4. Cyst phantom imaging without noise.

region and the mean power of background area [26]. Standard deviation represents the robustness of algorithms, the smaller the standard deviation is, and the better the robustness is [27]. Contrast noise ratio (CNR) is the quotient of CR and standard deviation.

As shown in the Tables 3 and 4, adaptive algorithms have better CR than traditional DAS without noise.

Compared with MV, the CR of ESBMV and LCMV is increased by 6.93 and 4.83 dB respectively. From the mean power of cyst region, it can be seen that LCMV has stronger noise suppression than ESBMV. However, the noise suppression in the background region of ESBMV is stronger than that of LCMV in the cyst area, resulting in a lower background mean power, so

Table 2. Mainlobe width at axial distance of 40 mm

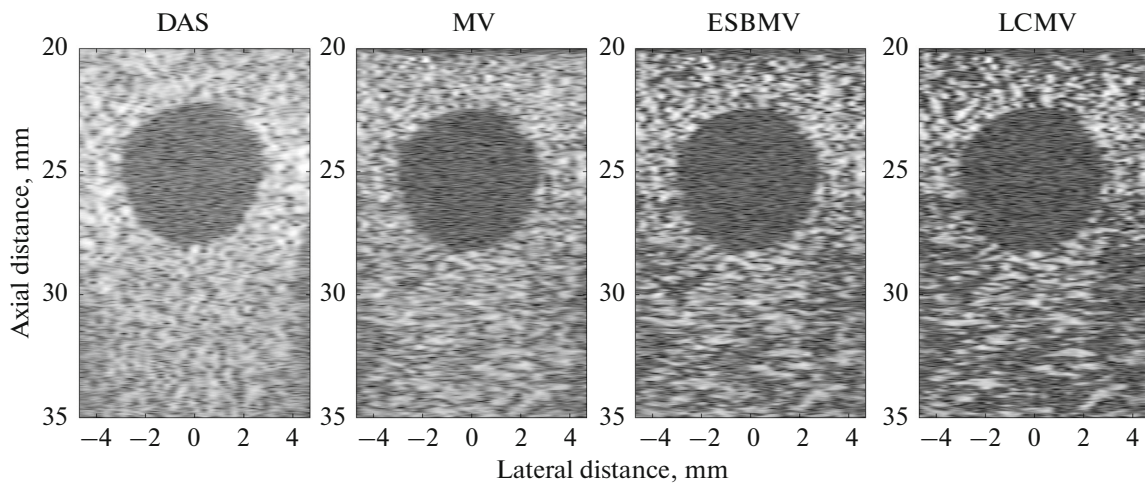| Methods	Mainlobe width (−dB)/mm		First sidelobe peak/dB	
	without noise	10 dB noise	without noise	10 dB noise
DAS	2.58	2.61	−18.46	−18.68
MV	1.70	1.88	−26.80	−25.68
ESBMV	1.67	1.76	−53.35	−37.48
LCMV	1.58	1.64	−52.65	−36.97

Fig. 5. Cyst phantom imaging with noise.

the CR of LCMV is slightly lower than that of ESBMV.

3.3. Different Center Frequencies Simulation

In the actual ultrasound detection, ultrasound probes with different center frequencies are often used according to different occasions. For example, the convex array probes used in abdominal test usually needs different frequencies of 2.5, 3.5 and 5.0 MHz. The intracavity probe is usually 6.5 MHz, and the linear probe for blood vessel detection is usually 7.5 MHz. In some special occasions, some high frequency linear probe can reach up to 10 MHz. In order to further inspect the proposed LCMV, 4 representative probe frequencies are selected for point target simulation, and the other parameters are the same with Table 1. The results are shown in Fig. 6.

From Fig. 6 we can see, the resolution of different algorithms is increased and the artifacts are decreased with the increase of center frequency. Compared with other methods, LCMV can maintain better performance at different center frequencies and can be suitable for different detection objects. The 5.0 MHz central frequency and 20.5 mm axial distance are selected for the lateral resolution analysis, and the result is shown in Fig. 7. As shown in Fig. 7, the resolution of adaptive algorithm is superior to traditional DAS.

Compared with MV and ESBMV, the proposed LCMV has the best resolution because of its narrowest mainlobe width and lowest sidelobe, which is consistent with the result of Fig. 6.

3.4. Algorithm Complexity Analysis

There are a lot of complex matrix operations in adaptive algorithms, whose complexity can be characterized by accumulating the complexity of matrix operations involved in algorithms. The complexity of common operations for N dimensional matrix is shown in Table 5.

It can be found from Table 5 that matrix inversion and eigenvalue decomposition have the highest complexity. DAS only involves matrix addition, so the complexity is $O(N)$. MV involves the inversion of the sub-array echo signal covariance matrix, and the complexity is $O(L^3)$. ESBMV includes the inversion of covariance matrix, eigenvalue decomposition, eigenvalue sorting and weighting vector projection operation. The complexity of ESBMV is $O(3L^3 + 2L^2)$. LCMV converts the inversion of reduced dimension covariance matrix into the vector multiplication. By improving the power method to obtain the maximum eigenvalue and corresponding eigenvector, the complexity of eigenvalue decomposition is reduced to

Table 3. Contrast ratio of cyst phantom imaging without noise

Methods	Mean power of cyst region/dB	Mean power of background region/dB	Standard deviation/dB	CR/dB	CNR
DAS	−41.89	−17.81	7.21	24.07	3.34
MV	−47.61	−22.85	8.14	24.75	3.04
ESBMV	−60.32	−28.64	12.87	31.68	2.46
LCMV	−61.96	−32.38	11.68	29.58	2.53

Table 4. Contrast ratio of cyst phantom imaging with noise

Methods	Mean power of cyst region/dB	Mean power of background region/dB	Standard deviation/dB	CR/dB	CNR
DAS	−27.35	−17.79	6.77	9.56	1.41
MV	−30.88	−22.14	7.16	8.74	1.22
ESBMV	−31.99	−24.92	8.44	7.07	0.84
LCMV	−34.08	−26.42	8.14	7.66	0.94

$O(N^2)$. Besides, the weighting vector projection operation is involved. Therefore, the computational complexity of LCMV is $O(3(p + 1)^2)$. In this paper, $N = 64$ is the number of elements, $L = 32$ is the number of sub-array elements after spatial smoothing. p is the dimension reduction parameter of sample covariance matrix. To select the optimal p, the MSE and efficiency with different p are given in Fig. 8.

As shown in Fig. 8, the dimension reduction parameter $p = 8$ can not only effectively reduce the complexity, but also narrow the difference between the dimension reduction data and the original data, thus ensuring the image quality of the LCMV algorithm.

Therefore, the proposed algorithm chooses $p = 8$. To further inspect the efficiency, the imaging time of point targets and cyst phantom are calculated in Table 6. The software platform is MATLAB R2017b, and the computer configuration is as follows: Intel i7-8700K 4GHz CPU, 8GB DDR-2400MHz.

The detection of the point targets ranges from 30 to 80 mm, and that of the cyst phantom is from 20 to 35 mm. The sampling points of the two objects are obviously different, so the imaging time of the point targets is longer than that of cyst phantom. As can be seen from Table 6, the imaging time of DAS is significantly less than that of adaptive algorithms due to its simple operation. Compared with MV, LCMV
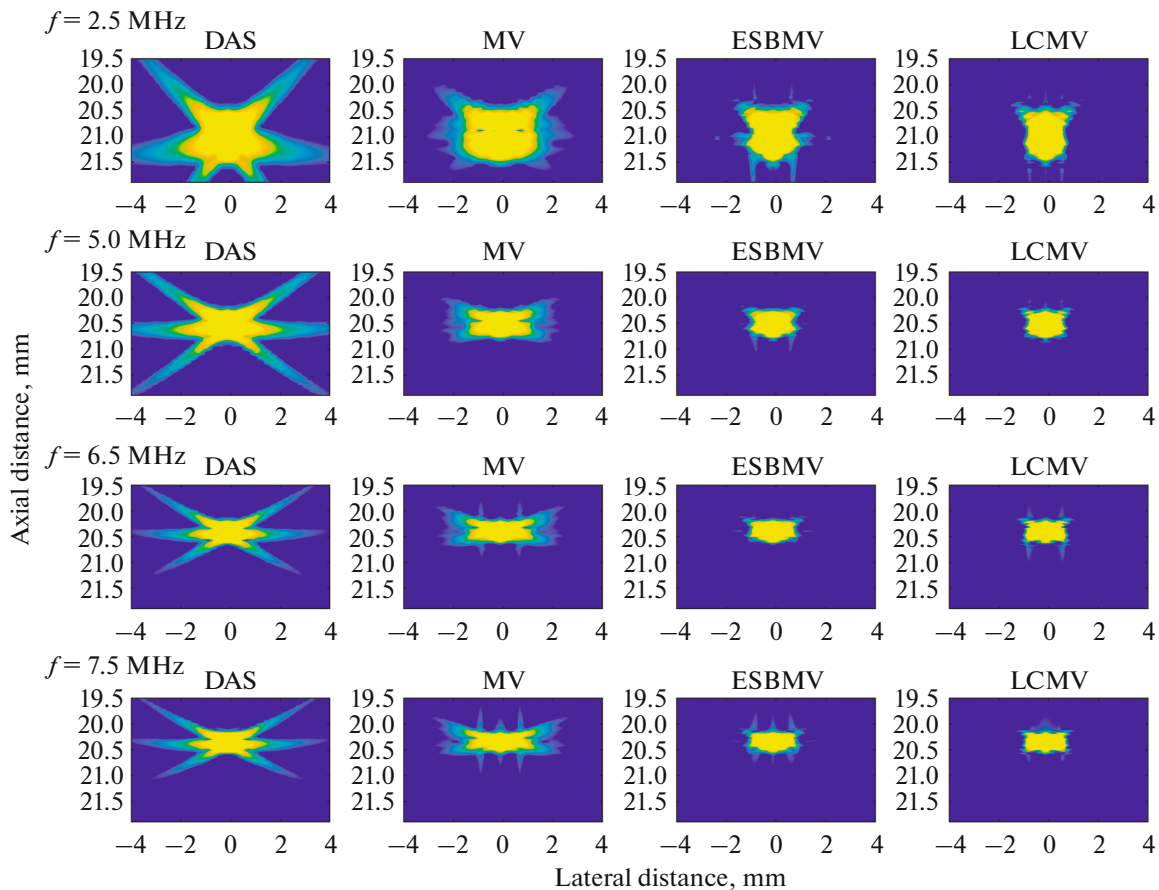
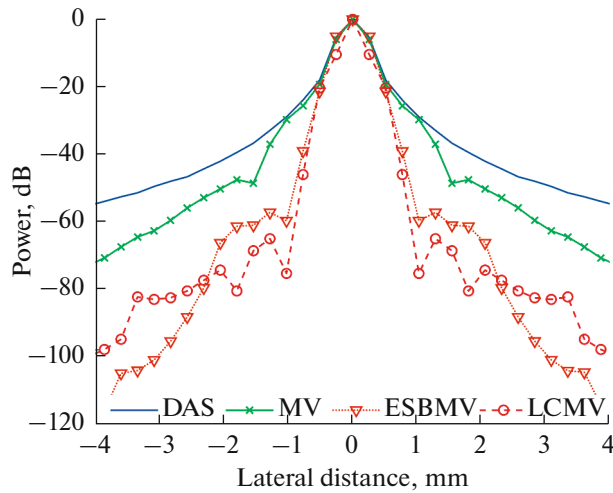
Fig. 6. The resolution of 5.0 MHz center frequency.

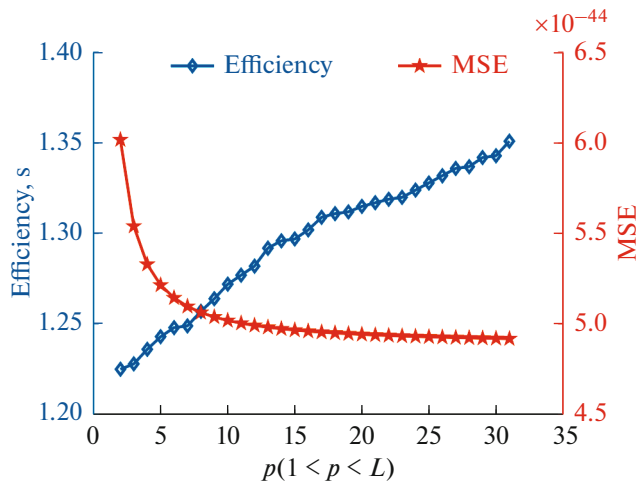**Fig. 7.** The comparison between different center frequencies.

Fig. 8. The efficiency and MSE with different p.

Table 5. The complexity of matrix operations

Matrix operations	Complexity levels
Matrix addition	$O(N)$
Eigenvalue sorting	$O(N^2)$
Vector multiplication	$O(N^2)$
Matrix inversion	$O(N^3)$
Eigenvalue decomposition	$O(N^3)$

Table 6. The comparison of imaging time

Methods	Efficiency/s	
	point targets	cyst phantom
DAS	2.61	1.12
MV	31.36	16.13
ESBMV	83.60	39.30
LCMV	23.86	11.67

reduces the dimension of covariance matrix, and simplifies the matrix inversion, so the imaging time of point targets and cyst phantom is reduced by 23.92 and 27.65% respectively. Compared with ESBMV, the imaging time of point target and cyst phantom is reduced by 71.46 and 70.31% respectively, because LCMV simplifies matrix inversion and eigenvalue decomposition.

4. CONCLUSION

A low-complexity minimum variance algorithm (LCMV) based on power method is proposed in this paper, which can further improve the image quality and reduce the complexity compared with traditional MV algorithm. The proposed algorithm can not only determine the dimension reduction parameters of covariance matrix based on ultrasonic echo data, but also can reduce the complexity of eigenvalue decomposition and matrix inversion by power method, which greatly improves the imaging efficiency.

The simulation experiments indicate that the LCMV algorithm has better resolution and efficiency than MV and ESBMV algorithm. Besides, the LCMV maintains lower artifacts and higher resolution than other mentioned algorithms at different center frequencies, which can be widely applied to different detection occasions.

REFERENCES

1. L. V. De, G. Szekely, and C. Tanner, Ultrasound Med. Biol. **41** (12), 3044 (2018).
2. R. S. Bandaru, A. R. Sornes, J. Hermans, E. Samset, and J. D'hooge, IEEE Trans. Ultrason., Ferroelectr. Freq. Control **63** (12), 2057 (2016).
3. M. Sorensen, I. Domanov, and L. L. De, IEEE Trans. Signal Process. **66** (14), 3665 (2018).
4. A. Hassanien and S. A. Vorobyov, IEEE Signal Process. Lett. **16** (1), 22 (2009).
5. C. C. Zheng, J. Cheng, and H. Peng, Acta Acust. **42** (1), 109 (2017).
6. J. Kortbek, J. A. Jensen, and K. L. Gammelmark, Ultrasonics **53** (1), 1 (2013).
7. C. C. Shen, Y. Q. Xing, and G. Jeng, Ultrasonics **72** (1), 177 (2016).
8. C. C. Zheng, H. Peng, and Z. H. Han, Acta Phys. Sin. **63** (14), 413 (2014).
9. L. N. Ribeiro, A. L. F. de Almeida, and J. C. M. Mota, Signal Process. **158** (1), 15 (2019).

10. P. Wang, Y. Z. Shi, J. Y. Jiang, L. Kong, and Z. H. Gong, Acoust. Phys. **65** (1), 123 (2019).

11. T. Dietzen, A. Spriet, W. Tirry, S. Doclo, M. Moonen, and W. T. Van, IEEE/ACM Trans. Audio Speech Lang. Process. **27** (3), 544 (2019).

12. P. Wang, Z. H. Gong, N. Cheng, and N. Li, Acta Acust. **42** (2), 214 (2017).

13. I. K. Holfort, F. Gran, and J. Jeonsen, IEEE Trans. Ultrason., Ferroelectr. Freq. Control **56** (2), 314 (2009).

14. P. Wang, N. Cheng, Z. H. Gong, and L. H. Wang, Acta Phys. Sin. **64** (23), 404 (2015).

15. J. K. Li, X. D. Chen, Y. Wang, Y. F. Shi, and D. Y. Yu, Acoust. Phys. **63** (2), 229 (2017).

16. T. Su, S. Zhang, D. Y. Li, and D. J. Yao, Acoust. Phys. **64** (3), 379 (2018).

17. Q. Wang, B. Zhou, Y. Chen, and H. Quan, Acoust. Phys. **65** (2), 226 (2019).

18. D. R. Fuhrmann, IEEE Trans. Signal Process. **39** (10), 2194 (1991).

19. J. Park, S. M. Wi, and J. S. Lee, IEEE Trans. Ultrason., Ferroelectr. Freq. Control **63** (2), 256 (2016).

20. K. Kim, S. Park, J. Kim, S. B. Park, and M. Bae, IEEE Trans. Ultrason., Ferroelectr. Freq. Control **61** (6), 930 (2014).

21. J. Yang, E. Grunsky, and Q. M. Cheng, Nat. Resour. Res. **28** (2), 431 (2019).

22. R. C. de Lamare and R. Sampaio-Neto, IEEE Trans. Veh. Technol. **59** (3), 1217 (2010).

23. M. Albulayli and D. Rakhmatov, in *Proc. 2013 IEEE Int. Conference on Acoustics, Speech, and Signal Processing (ICASSP)* (Vancouver, 2013), p. 1061.

24. A. M. Deylami and B. M. Asl, Ultrasonics **66** (1), 43 (2016).

25. L. Candemir and I. Cilesiz, in *Proc. 2008 Medical Imaging 2008: Physics of Medical Imaging (SPIE)* (San Diego, CA, 2008), p. 6913.

26. K. Ranganathan and W. F. Walker, IEEE Trans. Ultrason., Ferroelectr. Freq. Control **54** (4), 782 (2007).

27. J. C. Tillett, J. P. Astheimer, and R. C. Waag, IEEE Trans. Ultrason., Ferroelectr. Freq. Control **57** (1), 214 (2010).